Minerals Engineering 72 (2015) 31–35

Contents lists available at ScienceDirect

Minerals Engineering

journal homepage: www.elsevier.com/locate/mineng

Technical note

Effect of entrainment in bubble load measurement on froth recovery estimation at industrial scale

J. Yianatos [a,*], L. Vinnett [a], C. Carrasco [a,b], M. Alvarez-Silva [a]

[a] Automation and Supervision Centre for Mining Industry, CASIM, Department of Chemical and Environmental Eng., Federico Santa Maria Technical University, P.O. Box 110-V, Valparaíso, Chile

[b] University of Queensland, Australia[1]

ARTICLE INFO

Article history:
Received 11 October 2013
Accepted 11 December 2014
Available online 5 January 2015

Keywords:
Froth recovery
Bubble load
Entrainment
Flotation

ABSTRACT

Froth recovery was calculated in a 130 m^3 mechanical cell of a rougher flotation circuit. This was done by bubble load determinations along with mass balance surveys. Valuable grade in the bubble load decreased in the −38 μm due to fine particles entrained to the chamber of the device. The effect of fine particle entrainment on froth recovery was evaluated. A comparison between results from the raw bubble load data (assuming all particles were transported by true flotation) with those from corrected bubble load information (subtracting fine particle entrainment) was carried out. Entrainment occurred due to hydraulic transport in the bubble rear, which corresponds to the worst case scenario for froth recovery estimation. Results showed that the relative error was less than 0.3%, which allowed validation of the bubble load measurement as an effective methodology for froth recovery estimation at industrial scale.

1. Introduction

Flotation has been used for more than a century to separate valuable mineral from gangue and it remains a major process for mineral concentration. In flotation, hydrophobic particles have the highest probabilities of attachment to bubbles to be transported to the concentrate streams. Thus, differences in hydrophobicity between the different minerals are necessary for a selective separation.

Bubble loading allows for the mineral collected by true flotation to be sampled. Bubble load knowledge can be used to develop strategies for increasing floatability of valuable minerals as well as the depression of gangue. Therefore, bubble load determination is important to understand the collection processes, which allows flotation parameters to be optimized. In addition, bubble load can be used to determine the contribution to the overall recovery of both collection and froth zones independently. Thus, the bubble load measurement is useful to evaluate froth recovery, which is affected by particle detachment, especially in scavenging operations (Runge et al., 2010).

Some researchers have reported work on the analytical modelling of bubble loading. For example, van Deventer et al. (2001) developed a model that allows bubble load to be estimated. Parameters such as concentration of species in the pulp, the flow rates of species in the concentrate and tailings, superficial air rate, air holdup, wash water rate and mineralogical liberation are required for the model evaluation. Besides requiring parameters that are often difficult to measure, analytical methods are usually based on assumptions which cannot be justified.

Devices for direct bubble load determinations have been reported in literature. As far as could be ascertained, most of these devices are only appropriate for laboratory scale flotation or applicable under specific industrial operation conditions. For instance, Bradshaw and O'Connor (1996) developed a method for bubble load measurements in laboratory scale cells. This method requires careful control of parameters such as bubble size, airline pressure and mineral preparation to obtain adequate reproducibility. Falutsu and Dobby (1992) presented a method to measure bubble load in flotation columns that consists of separating the solids carried by the bubbles from the solids dispersed in the slurry. This approach does not account for the detachment of particles and the rejection of fine particles (the sampler was operated with a downward water bias velocity several times greater than the superficial gas velocity). However, this device was one of the first apparatus to directly measure bubble-load in industrial mechanical cells. Dyer (1995) developed a device that uses the positive displacement principle (i.e., there is a net downward flow of water). The sensor measures bubble load by collecting mineralized bubbles by a riser tube. After bubbles burst, particles are accumulated in a chamber during a period of time. The air then pushes down the

* Corresponding author.
E-mail address: juan.yianatos@usm.cl (J. Yianatos).
[1] Present address.

http://dx.doi.org/10.1016/j.mineng.2014.12.017
0892-6875/

water that initially filled the chamber. The displaced water flows down the riser avoiding suspended particles to be sampled. Bubble load (g/L) is determined by correcting the volume of the gas for hydrostatic pressure effects. Despite its simplicity, Bhondayi (2010) found that this device did not produce satisfactory bubble load measurements due to particle losses in the riser. Seaman et al. (2004) developed an apparatus similar in concept to the one developed by Dyer (1995). This device regulates the liquid bias by the size of a nozzle. It is claimed that the nozzle also helps to reduce the entrainment in the riser (Seaman et al., 2004). Industrial practice showed that suitable reproducibility can be obtained with this device. One of the limitations of this method is the possibility of true floated fine particles detach following streamlines down the riser with the displaced water (Bhondayi and Moys, 2011). Rahman et al. (2010, 2013) developed a special column which consists in two concentric tubes. The outer tube goes from the top of the froth to the sampling point in the pulp; the inner tube that goes from the pulp–froth interface and acts as a drop back collector, in which bottom part is connected to a reservoir for the detached particles. Although this device has shown adequate reproducibility in plant operations, it has some limitations related to wall effects and it is still under development.

The apparatus developed by Dyer (1995) and improved by Moys et al. (2010), has been industrially tested with remarkable reproducibility (Yianatos et al., 2008). To ensure reliable bubble load determinations, the device must ensure: (i) no particle losses from the bubble-particle aggregate into the sampling tube, (ii) no suspended particles entrained from the collection zone to the bubble load chamber. Otherwise, the bubble load sensor might yield to biased results. Thus, a special attention to the flow regime developed in the sampling tube must be taken into account.

In this technical note, bubble load measurements in the first cell of a rougher circuit were carried out per size classes. In parallel, mass balances were carried out to determine froth recovery. Cyclosizer analyses of the bubble load samples in the fine classes showed a Cu grade decrease for particles under 38 μm. Thus, the presence of floatable (pyrite) and non-floatable (insoluble) gangue in the bubble load sensor was studied. In addition, the objective of this work was to evaluate the effectiveness of the bubble load device developed by Moys et al., (2010) to estimate froth recovery under entrainment condition. The impact of fine gangue in the bubble load samples on the froth recovery estimation was studied.

2. Plant surveys

The plant work consisted of sampling for mass balances around a rougher flotation bank from El Teniente concentrator, Codelco-Chile. The rougher circuit consists of four parallel banks of seven 130 m^3 mechanical cells in a 1–2–2–2 arrangement (Carrasco, 2010). Data from two surveys in the first rougher cell were employed. The sampling points are shown in Fig. 1.

The metallurgical data was classified into two size fractions (−45 μm and +45 μm) and assayed for copper, molybdenum and iron (by acid digestion followed by atomic absorption spectroscopy). Grade data were reconciled to satisfy the total and component mass balances around the first cell. Additional measurements, such as bubble load and superficial gas rate were carried out in this cell according to the experimental procedure described by Yianatos et al., (2008). Table 1 shows the operating conditions of the rougher circuit during the surveys.

Bubble load samples were classified into nine class fractions and assayed for Cu, Mo and Fe. Insolubles (silicates) were also analyzed. Each size class was reported as the following mean sizes: 208 μm, 104 μm, 57 μm, 38 μm, 28 μm, 20 μm, 14 μm, 10 μm and 8 μm. The fraction under 45 μm was classified by the Cyclosizer system.

3. Measurements and results

Table 2 shows an example of the reconciled grade data per size class (Cu, Mo and Fe) around the first rougher cell during Survey 1. The mass balance adjustment results allowed the concentrate mass flowrate (94 tph) and the Cu concentrate grade per size class to be identified.

In order to estimate the froth recovery, the mass transport of floatable mineral across the pulp–froth interface must be known. This material entering the froth is calculated by measuring the bubble load, the superficial gas rate and the cell cross-sectional area at the interface level. The superficial gas rate, J_G, was measured at the pulp–froth interface level of the mechanical cell. The bubble load device was used as a J_G sensor, with the volumetric displacement of liquid over time being used to obtain the volumetric gas flowrate. The range of superficial gas rates in mechanical cells at a local pressure of 80 kPa, 1700 masl, was J_G = 1.2–1.4 cm/s.

Fig. 2(a) and (b) shows the USM bubble load sensor and the sampling point in the industrial cell, respectively. This device is

Table 1
Plant conditions in the feed rougher flotation circuit (sampling point 1) during the metallurgical surveys.

	Survey 1	Survey 2
Feed flowrate per bank, tph (1)	726	708
Cu grade, %	1.01	0.96
Fe grade, %	4.47	4.58
Mo grade, %	0.021	0.020
Solid percentage, %	41	39
pH	9.4	9.5

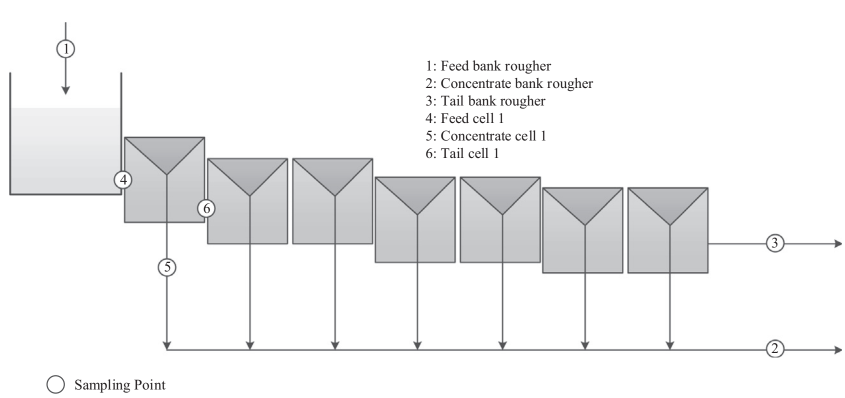

Fig. 1. Arrangement and sampling point in the first rougher cell and the bank (Carrasco, 2010).